

Original Article

Modified Whale Optimization Algorithm with Deep Learning-Driven Plant Leaf Disease Detection and Classification

N. Venkatakrishnan¹, M. Natarajan²

^{1,2}Department of Computer and Information Science, Annamalai University, Annamalai Nagar, Chidambaram, India.

¹Corresponding Author : narayanav175@gmail.com

Received: 21 September 2023

Revised: 20 December 2023

Accepted: 01 April 2024

Published: 24 April 2024

Abstract - Plant Leaf Disease (PLD) cause extensive damage to crops, resulting in economic losses and reduced yields in agriculture. For timely intervention and effective disease management, earlier identification of these diseases is significant. Recently, the Deep Learning (DL) technique has had tremendous potential in the fields of Computer Vision (CV), involving recognition and classification of PLD. Researchers and developers have been capable of achieving tremendous performance in the identification and classification of PLDs by leveraging Deep Neural Networks (DNN), which aids in earlier diagnosis and intervention. This study offers a Modified Whale Optimization Algorithm with DL-Driven PLD Detection and Classification (MWOADL-PLDDC) technique. The MWOADL-PLDDC technique leverages the DL model with a hyperparameter tuning strategy for recognizing PLD. To obtain this, the MWOADL-PLDDC technique makes use of the Multi-Direction and Location Distribution of Pixels in Trend Structure (MDLDPTS) technique for feature extraction purposes. Meanwhile, the Deep Stacked Autoencoder (DSAE) method gets exploited for the recognition of healthy and diseased plant leaf images. For enhancing the detection rate of the DSAE approach, the IWOA is utilized to alter the hyperparameter value of the DSAE approach. The simulation outcomes demonstrate the efficacy of the MWOADL-PLDDC technique in the accurate recognition and classification of PLDs. The MWOADL-PLDDC technique exhibits high accuracy in distinguishing healthy leaves from diseased ones and accurately identifying the specific disease type.

Keywords - Image classification, Deep learning, Plant leaf disease, Computer vision, Convolutional whale optimization algorithm.

1. Introduction

PLD was liable for reducing crop productivity, which can affect the food production systems globally, leading to economic loss. PLDs and pests are accountable for around 20-40% reduction in global food productivity based on the report of the Food and Agriculture Organization (FAO) [1]. Globally, plant ailments are accountable for an approximated value of 13% of reduction in crop productivity. These statistical values highlighted the significance of recognizing plant diseases to eliminate crop reduction. Nevertheless, it is essential to realize the factors accountable for plant disease [2]. There are three factors supporting the disease development in the plants such as favourable environment, pathogen, and host [3]. In many conditions, diseases start to indicate signs and affect the plants from the bottom-up order and several PLDs spread out all over the crop after infections. Hence, crops are required to be observed continuously as primarily managing the disease will support in avoiding the spreading [4]. In many scenarios, plant disease also emerges in the season after they are pollinated. Efficient plant disease

detection includes recognition of several diseases in various crops and many concurrent diseases, primary-season plant disease recognition, approximating the seriousness of the diseases, useful measures to carry for managing the disease to restrict its spread out and estimating the applicable volume of pesticides [5]. Image-based plant disease recognition is the latest investigating field by numerous research workers [6]. Since crop or yield wastage is raising because of diseases, it becomes essential to recognize the diseases efficiently within a particular time [7]. In growing countries, specifically in South Asia majority of the population is based on farming indirectly or directly, in countries are becoming significant to make use of applications based on detecting vegetation ailments that can support cultivators to know the causes of diseases and also receive the prevention to handle them [8]. Early recognition of PLD based on the leaf colour, development of the pattern and size of the leaf, etc., can be useful to the cultivators. Machine Learning (ML) was initiated to obtain an interest in plant disease recognition about 20 years ago when its implementations were considered and



investigations were examined for plant diseases and agriculture. Conventional ML methods were commonly used in research communities for recognizing plant diseases [9]. Few classical ML methods were utilized for the detection of plant ailments, including SVM for detecting tomato disease, detection of K-Nearest Neighbour (KNN) for soybean disease, and detection of random forests for tomato disease. DL is a subcategory of ML [10]; it has become a preferred method for the detection of diseases because of improved computational abilities, power, availability, and storage of huge amounts of databases.

This study suggests a Modified Whale Optimization Algorithm with DL-Driven PLD Detection and Classification (MWOADL-PLDDC) method. The MWOADL-PLDDC approach makes use of the Multi-Direction and Location Distribution of Pixels in Trend Structure (MDLDPTS) approach for feature extraction purposes. Meanwhile, the Deep Stacked Autoencoder (DSAE) technique gets exploited for the recognition of healthy and diseased plant leaf images. For enhancing the detection rate of the DSAE approach, the IWOA is utilized to alter the hyperparameter value of the DSAE approach. The simulation outcomes demonstrate the efficacy of the MWOADL-PLDDC technique in the accurate recognition and classification of PLDs.

2. Related Works

In [11], a new image processing method and multiple class SVM are utilized to identify and classify the diseases of grape leaves. In this study, SVM was utilized as a robust classification algorithm, where PCA was implemented for the reduction of feature dimension. Lastly, the relevant feature was chosen by selecting relief features. In [12], the study adopted an ML method for the earlier diagnosis of grape leaf diseases and precisely differentiated between dissimilar classes of diseases. Moreover, the CNN-based Classification (CNNC) algorithm and KNN are proposed for classifying PLDs. Next, the classification technique is implemented on the high-quality gradient-based feature. Hossain et al. [13] examined a technique for recognizing and classifying the PLD utilizing the KNN approach. The texture feature was extracted in leaf images for classification.

In [14], four modified DL algorithms are introduced for classifying and recognizing grape leaf disease based on grape leaf datasets. In this study, the TL model was utilized based on three pre-trained ML architectures (VGG16, AlexNet, and MobileNet). Lilhore et al. [15] give a wide-ranging learning model for the real-time recognition of Cassava leaf disease dependent upon Enhanced CNN (ECNN). The typical CNN architecture exploits data pre-processing features, which increases the computation overheads. A depthwise convolution was used to resolve the CNN issue in the ECNN algorithm. Singh et al. [16] introduce a strategy employing an enhanced CNN (ECNN) technique.

Here, gamma correction, distinct block processing, and global average election polling with batch normalizing features are utilized. In [17], the author introduced a DL-based approach for classifying and detecting plant disease in leaf imageries taken in various resolutions. A compact CNN model was trained on larger images of plant leaves data from several countries. Images with different inter-and-intra-class variants have challenging and complex environments that are addressed in these Dense NN models.

3. The Proposed Model

In this paper, a novel PLD detection system is established, named the MWOADL-PLDDC method. The MWOADL-PLDDC technique leverages the DL model with a tuning strategy for PLD recognition. It comprises three stages such as MDLDPTS feature extractor, IWOA and DSAE based tuning and classification. Figure 1 portrays the complete workflow of the MWOADL-PLDDC methodology.

3.1. Design of MDLDPTS Model

The presented work combined MDLDPTS that efficiently represents data variation of pixels, local design's spatial procedure, and relation amid local-level structure as large\equal\small trends of colour, shape, and texture data, but equal trend represents the same intensity values, small and large trend refers to the intensity values in large to small, and vice versa [18]. Moreover, the MDLDPTS also encrypts the average place for the pixel value distribution to the overall trends from the local-level structure, and to utilize the model, RGB imageries are changed as HSV colour spacing next colour quantized on S , V , and H texture quantized on V and edge quantized on Sobel function executed V element imagery can be carried out and the levels of quantized were fixed to 108, 20, 9 for the data of colour, texture, and edge correspondingly. The local structure to all the 3x3 non-overlapping sub-images can be recognized to all each colour\texture\edge quantization data from the procedure of trends. MDLDPTS is signified as matrix output of colour\texture\edge vs. average place for dispersion of pixels of large\equal\small trends to the overall orientations. The calculated aspects of colour, texture, and edge for trend formation and its positionings are shown as:

$$F_{\theta} = \{(\theta_E^{Q_c}, \theta_S^{Q_c}, \theta_L^{Q_c}), (\theta_E^{Q_e}, \theta_S^{Q_e}, \theta_L^{Q_e}), (\theta_E^{Q_t}, \theta_S^{Q_t}, \theta_L^{Q_t})\} \quad (1)$$

Whereas orientation $(\theta) \in \{0^\circ, 45^\circ, 90^\circ, 135^\circ\}$, quantization edge value $(Q_e) \in \{1, 2, \dots, 9\}$, colour values quantized $(Q_c) \in \{1, 2, \dots, 108\}$, quantization texture value $(Q_t) \in \{1, 2, \dots, 20\}$, L , E , and S represent the large, equal, and small trends structures correspondingly, and $\theta_E^{Q_c}$, $\theta_S^{Q_e}$ and $\theta_L^{Q_t}$ portrays the orientation of equal trend structure for Q_c , Q_e and Q_t , and the size of matrices are 108x4, 9x4, and 20x4 correspondingly. The calculated average place for the distribution of pixels for trends structure was depicted as:

$$F_{\mu} = \{(\mu_{E\theta}^{Q_c}, \mu_{S\theta}^{Q_c}, \mu_{L\theta}^{Q_c}), (\mu_{E\theta}^{Q_e}, \mu_{S\theta}^{Q_e}, \mu_{L\theta}^{Q_e}), (\mu_{E\theta}^{Q_t}, \mu_{S\theta}^{Q_t}, \mu_{L\theta}^{Q_t})\} \quad (2)$$

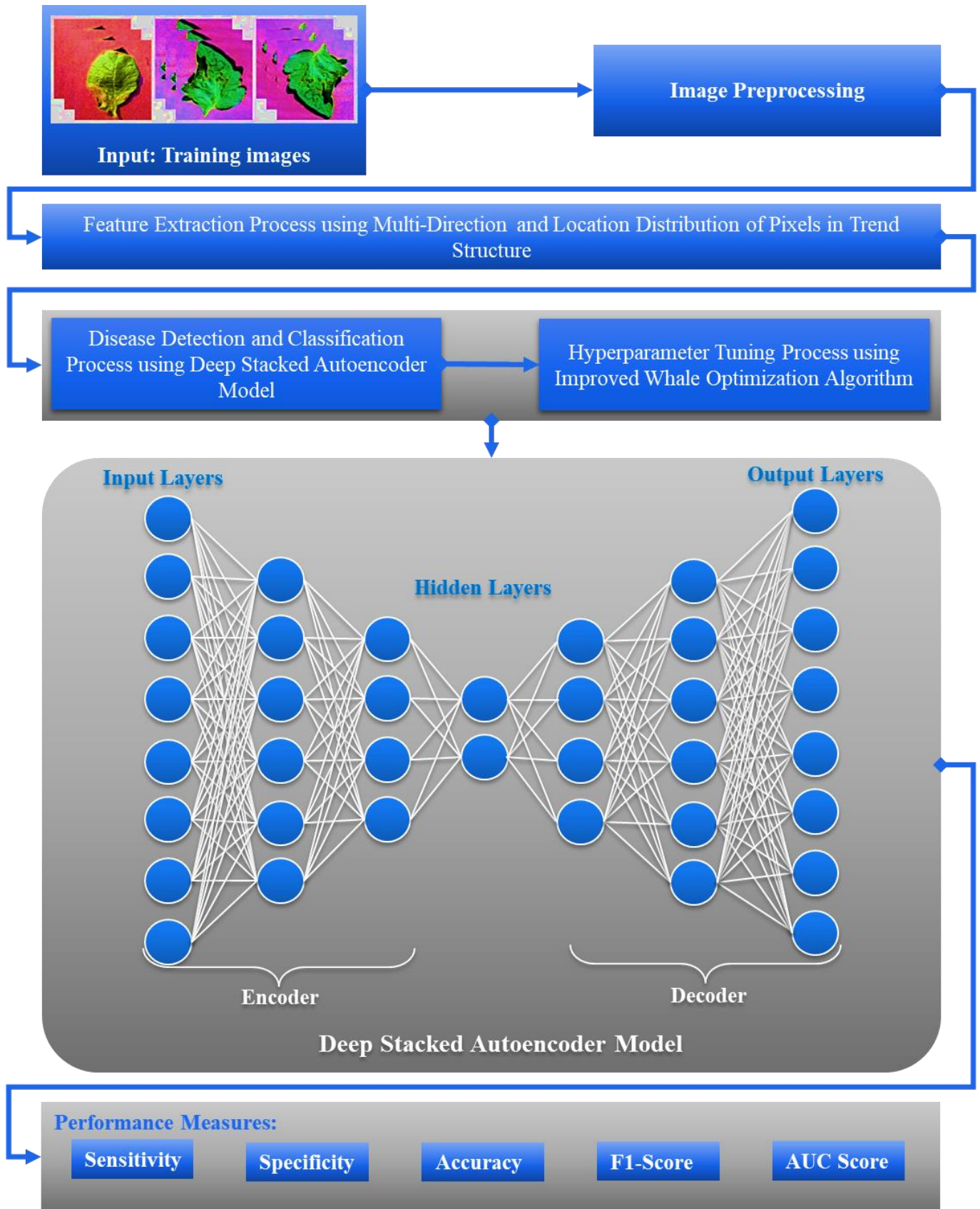


Fig. 1 Overall flow of MWOADL-PLDDC approach

Whereas μ illustrates the average place for the pixel value distribution, $\mu_{E\theta}^{Q_c}$, $\mu_{E\theta}^{Q_e}$ and $\mu_{E\theta}^{Q_t}$ imply the average place for the pixel dispersion at orientation θ of equal trend structures for Q_c , Q_e and Q_t respectively. The estimate of μ in each local trends structure is as follows:

$$\mu = \frac{1}{M} \sum_{i=0}^M P_i \quad (3)$$

Whereas P and M indicate the pixels and count of intensity values from the trend structure. Therefore, the MDLDPTS is determined as follows:

$$F = \{F_\theta, F_\mu\} \quad (4)$$

3.2. Plant Disease Detection using DSAE Model

The DSAE model is used for the detection of PLD in this work. The Autoencoder (AE) method is a type of unsupervised NN which comprises encoding and decoding parts [19]. In the encoder phase, the implied property of the input data can be studied, and in the decoder phase, the input data is reproduced by using novel features which are studied.

The encoder's output of the HL features, named as coding feature, can be considered as a representation of data D , which is inputted into the encoding part. Simultaneously, the features of the HL are the features that can be attained using the reduction dimensional of the encoding part. In such cases, the data of HL H have small dimensional than the data of D and D_o input and the output layers; this can be given by the detail that $|D|$ is higher than $|H|$, $|D_o|$, and $|D|$ was equivalent to $|D_o|$. Firstly, compute H utilizing the mapping matrix $= x(D)$ that takes from the D input layer to H HLs. Then, evaluate D_o by the map matrix $D_o = y(H)$ that takes from the H HLs to the D_o output layer.

$$\begin{aligned} x: \alpha &\rightarrow \delta \\ y: \delta &\rightarrow \alpha \\ x, y &= \arg \min_{x, y} ||D - y[x(D)]||^2 \end{aligned} \quad (5)$$

Where δ denotes the magnitude of hidden space, α refers to the embedding input space (outcome space). The input space, characteristic space represented as D , H refers to the component of α , δ and is transmitted to the self-encoder, and the objective is to resolve the map (x, y) that presents among the 2 spaces to reduce the reconstructed error of input features.

It is also possible that a single AE is capable of decreasing the dimensionality of the input feature. The DSAE works based on the following principles.

- Train the initial AE dependent upon the input dataset and later obtain the feature vectors that are studied.
- The feature vector in the prior layer was employed as the layer's input, and this procedure lasted until the training was completed.
- The Backpropagation (BP) model is used after the HL has

been trained for performing fine-tuning. This can be obtained by updating the weights and reducing the cost function using a labelled training set.

3.3. Hyperparameter Tuning using IWOA

The IWOA is used to improve the detection outcomes of the DSAE algorithm. The WOA mimics humpback whales' haunting demeanours. The algorithm comprises the exploration and exploitation phases [20]. Exploration is the procedure of finding prey.

The given equation describes the encircling behaviours of humpback whales during hunting prey. The leading solution is considered the target prey. The residual solution attempts to end the aimed prey.

$$\vec{V} = |\sigma \cdot \vec{Y}_a(s) - \vec{Y}(s)| \quad (6)$$

$$\vec{Y}(s + 1) = |\vec{Y}_a(s) - \vec{\lambda} \cdot \vec{V}| \quad (7)$$

Whereas \vec{Y}_a denotes the optimal solution, v shows the existing iteration, the coefficient vector was σ and $\vec{\lambda}$

$$\vec{\lambda} = 2\vec{b} \cdot \vec{q} - \vec{a} \quad (8)$$

$$\vec{\sigma} = 2 \cdot \vec{q} \quad (9)$$

Where $(0,1)q$ represents the random vector, and \vec{b} denotes the linear reduce coefficient from two to zero. By implementing $\vec{\lambda}$ and $\vec{\sigma}$ vectors in the existing location, different locations are compared to the optimum solution and are controlled. Assume that the optimum solution is prey by using Eq. (7), variations in whales' existing location closer to the prey, and simulate that situation where the prey was encircled. The 2 mathematical modeling are defined, which mimics the humpback whale BubbleNet attacks.

1. Shrinking encircling strategy: The vector \vec{b} declined linearly. The co-efficient vector, a fluctuation limit dependent upon the arbitrary vector q , b is within $(-\vec{\lambda}, \vec{\lambda})$, \vec{b} declined from two to zero.
2. Spiral upgrade location: The humpback whale encircles the food source in a motion logarithmic spiral afterwards, the 1st method defines the length between self and prey.

$$\vec{Y}(s + 1) = \vec{V} \times f^{\mu\delta} \times \cos(2\omega\delta) + \vec{Y}_a(s) \quad (10)$$

The distance among humpback whales, as well as their prey, is characterized as $\vec{V} = |\vec{Y}_a(s) - \vec{Y}(s)|$. In $[-1,1]\delta$, is an arbitrary number. μ is constant and defines that the logarithmic spiral will be looked at. In the exploitation stage, when the prey position is defined, the humpback whale dives deep in to generate spiral-like bubbles nearby the food source and later moves upward towards the surface. During the iteration method, the hunting behaviour assumes that the spiral-structured path and the shrinking circle have the same implementation probability for updating the humpback whale location.

WOA selects the reference solution through a $\vec{\lambda}$ arbitrary vector value, which is lesser than -1 or greater than +1.

$$\vec{V} = |\sigma \cdot \overrightarrow{Y_{rand}} - \vec{V}| \tag{11}$$

$$\overrightarrow{Y}(s + 1) = \overrightarrow{Y_{rand}} - \vec{\lambda} \cdot \vec{V} \tag{12}$$

Where $\overrightarrow{Y_{rand}}$ denotes the location vector of the solution that is randomly chosen from the existing population.

The co-efficient vector $\vec{\lambda}$ allows a shift between exploitation as well as exploration. If $|\vec{\lambda}| > 1$ exploration was implemented, and if $|\vec{\lambda}| < 1$, then exploration was performed. WOA has the potential to switch between spiral-shaped paths and reduce circles during the exploitation stage. Although the WOA was extensively used to resolve different engineering problems, it has the problem of low calculation accuracy and slow convergence rate while handling complicated optimizer problems [21]. In this study, an IWOA was introduced to overcome this challenge, where the equal pitch Archimedean spiral curve and self-adaptive inertia weight are extra to the original WOA for improving the performance:

$$iw = iw_{max} - (iw_{max} - iw_{min}) \left(\frac{t}{T_{max}}\right)^{\frac{1}{t}} \tag{13}$$

In Eq. (13), iw_{max} and iw_{min} indicate maximal and minimal inertia weights, correspondingly and T_{max} indicates the maximal amount of iteration.

$$= \begin{cases} iw \cdot Y^*(t) - A \cdot |2r \cdot Y^*(t) - Y(t)|, & p < 0.5 \\ iw \cdot Y^*(t) + |Y^*(t) - Y(t)| \cdot e^{bl} \cdot \cos(2\pi l), & p \geq 0.5 \end{cases} \tag{14}$$

It can be notable in Equation (11), in which the inertia weight non-linearly reduces with the increasing iteration.

Initially, the inertia weight is larger; hence, the model consists of a better global searching capability, making the whale rapidly approaching the near prey region (fittest solution).

These principles are for the 2D case, where the location (y_1, y_2) of humpback whales is updated based on the present optimum location (y_1^*, y_2^*) . Any position near the optimum whale might be different by shifting the coefficient variables of a and r values. Due to poor algorithm periodicity, when the pitch of the spiral curve is smaller than the humpback whales, any region couldn't be searched. The Archimedean spiral curve is used to replace the logarithmic spiral curve from the WOA:

$$\begin{cases} y_1 = (a_0 + b \cdot l) \cos(2\pi l) \\ y_2 = (a_0 + b \cdot l) \sin(2\pi l) \end{cases} \tag{15}$$

Where $a_0 = 0$ and $b = 1$ is an instance of the Archimedean spiral curve. The pitch of spiral curves is a fixed value that could be changed simply to attain optimum accuracy.

$$= \begin{cases} iw \cdot Y^*(t) - A \cdot |2r \cdot Y^*(t) - Y(t)|, & p < 0.5 \\ iw \cdot Y^*(t) + |Y^*(t) - Y(t)| \cdot (a_0 + b \cdot l) \cdot \cos(2\pi l), & p \geq 0.5 \end{cases} \tag{16}$$

The fitness function is a main aspect of the IWOA approach. An encoder solution was implemented for estimating the best candidate solutions. Here, the accuracy output is the key condition utilized for scheming a FF.

$$Fitness = \max(P) \tag{17}$$

$$P = \frac{TP}{TP + FP} \tag{18}$$

Where TP and FP signify the true and the false positive values.

Table 1. Dataset description

Classes	Image Numbers	Classes	Image Numbers
	ALD		TLD
Healthy	554	BS	3404
BR	199	EB	2886
Scab	221	Healthy	516
CAR	99	LB	3769
	CLD	LM	2195
PM	409	SLS	1331
Healthy	334	SM	2251
	CPLD	TS	2195
CLS	187	MV	2411
CR	432	YLCV	2144
Healthy	354		PLD
NLB	433	BS	1377
	GLD	Healthy	1372
BR	407		PTLD
LB	465	EB	1377
Healthy	146	LB	1372
Esca	379	Healthy	193

4. Results and Discussion

In the present section, the investigational assessment of the MWOADL-PLDDC method was investigated utilizing different PLD datasets [22] such as apple, cherry, corn plant, tomato, grapes, pepper, and potato consisting classes such as Septoria Leaf Spot (SLS), Late Blight (LB), Early Blight (EB), Leaf Mold (LM), Common Rust (CR), Bacterial Spot (BS), Powdery Mildew (PM), Target Spot (TS), Spider Mites (SM), Mosaic Virus (MV), Yellow Leaf Curl Virus (YLCV), Cedar Apple Rust (CAR), Healthy, Northern LB (NLB), Esca, Cercospora-LS (CLS), Leaf Blight (LB), and Black Rot (BR). Figure 2 displays the image samples. An overall PLD detection output of the MWOADL-PLDDC methodology is tested under various datasets in Table 2. The results portrayed that the MWOADL-PLDDC methodology categorizes several class labels on all datasets. On the Apple Leaves Dataset (ALD), the MWOADL-PLDDC approach reaches average $sens_y$, $spec_y$, $accu_y$, $F1_{score}$, and AUC of 99%, 98.99%, 99%, 98.99%, and 99.62% respectively.

At the same time, on the Cherry Leaves Dataset (CLD), the MWOADL-PLDDC approach obtains average $sens_y$, $spec_y$, $accu_y$, $F1_{score}$, and AUC of 99%, 99%, 99.65%, 99%, and 99.23% correspondingly. Simultaneously, on the Corn Plant Leaves Dataset (CPLD), the MWOADL-PLDDC technique obtains average $sens_y$, $spec_y$, $accu_y$, $F1_{score}$, and AUC of 97.47%, 97.43%, 97.50%, 97.36%, and 97.15% correspondingly. Concurrently, on the Grape Leaves Dataset (GLD), the MWOADL-PLDDC technique attains average $sens_y$, $spec_y$, $accu_y$, $F1_{score}$, and AUC of 96.30%, 96.26%, 97.60%, 96.50%, and 96.35% respectively. Similarly, on the Pepper Leaves Dataset (PLD), the MWOADL-PLDDC method obtains an average $sens_y$, $spec_y$, $accu_y$, $F1_{score}$, and AUC of 95.74%, 95.86%, 99.62%, 95.88%, and 97.09% correspondingly. Lastly, on the Potato Leaves Dataset (PTLD), the MWOADL-PLDDC method obtains average $sens_y$, $spec_y$, $accu_y$, $F1_{score}$, and AUC of 95.75%, 95.86%, 95.90%, 95.89%, and 96.04% subsequently.

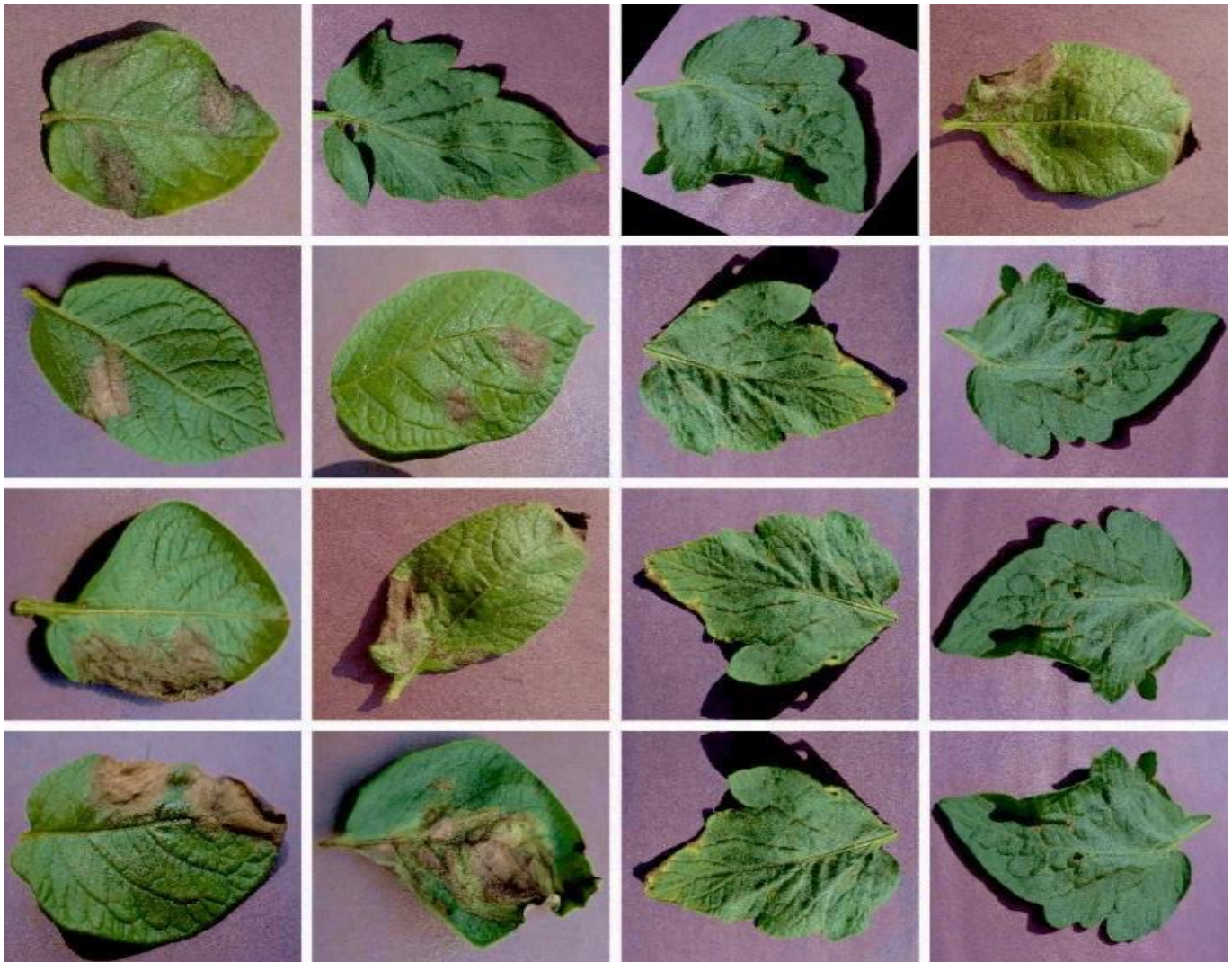


Fig. 2 Sample images

Table 2. PLD detection outcome of MWOADL-PLDDC method under diverse datasets

Classes	$Sens_y$	$Spec_y$	$Accu_y$	$F1_{Score}$	AUC
ALD					
Healthy	99.00	98.99	98.99	98.99	99.61
BR	99.00	98.99	99.00	98.99	99.62
Scab	98.99	98.99	99.00	98.99	99.60
CAR	99.00	99.00	99.00	98.99	99.65
Average	99.00	98.99	99.00	98.99	99.62
CLD					
PM	98.99	99.00	99.70	99.00	99.25
Healthy	99.00	99.00	99.60	99.00	99.20
Average	99.00	99.00	99.65	99.00	99.23
CPLD					
CLS	97.61	97.05	97.52	96.95	97.84
CR	97.60	97.54	97.78	97.29	96.96
Healthy	96.96	97.59	97.56	97.38	96.90
NLB	97.69	97.52	97.12	97.82	96.91
Average	97.47	97.43	97.50	97.36	97.15
GLD					
BR	96.43	96.13	97.19	96.60	96.19
LB	96.44	96.14	97.47	96.52	96.47
Healthy	96.27	96.40	97.32	96.56	96.32
Esca	96.05	96.37	98.41	96.32	96.41
Average	96.30	96.26	97.60	96.50	96.35
PLD					
BS	95.70	95.79	99.64	95.90	97.10
Healthy	95.77	95.92	99.60	95.85	97.07
Average	95.74	95.86	99.62	95.88	97.09
PTLD					
EB	95.71	95.87	95.97	95.91	95.99
LB	95.80	95.91	95.93	95.91	96.10
Healthy	95.73	95.80	95.79	95.86	96.02
Average	95.75	95.86	95.90	95.89	96.04
TLD					
BS	93.94	94.37	93.06	93.88	95.04
EB	94.60	93.76	93.02	93.44	95.09
Healthy	94.31	94.23	93.20	94.32	95.05
LB	93.42	94.44	93.50	94.36	95.08
LM	93.25	93.95	94.20	93.15	95.08
SLS	94.99	94.86	93.13	94.45	95.04
SM	93.80	94.22	93.33	93.65	95.09
TS	94.04	93.77	93.62	94.66	95.07
MV	92.99	94.60	93.09	94.90	95.07
YLCV	93.06	93.29	93.03	93.26	95.00
Average	93.47	93.97	93.27	94.12	95.06

Table 3. Relative outcome of MWOADL-PLDDC model with other methods under diverse datasets

Classifier		NB	RBFNN	FkNN	DT	SOM	RF	SVM	Fuzzy_SVM	MWOADL-PLDDC
Apple	CACC	90.10	92.40	95.90	96.50	97.10	97.80	98.40	98.90	99.00
	AUC	93.70	94.50	97.60	98.00	98.40	98.90	99.20	99.50	99.62
Cherry	CACC	95.10	95.90	97.70	97.90	98.50	98.90	99.20	99.50	99.65
	AUC	93.20	94.70	96.50	96.90	97.40	98.00	98.50	99.10	99.23
Corn	CACC	90.90	91.40	92.80	93.30	93.80	94.50	94.90	95.60	97.50
	AUC	91.80	92.20	93.70	94.30	94.70	95.50	96.10	96.70	97.15
Grapes	CACC	92.70	93.30	94.90	95.30	95.70	96.30	96.70	97.10	97.60
	AUC	90.60	91.80	92.70	93.30	93.70	94.40	95.10	95.90	96.35
Pepper	CACC	95.10	95.70	97.30	97.70	98.30	98.80	99.10	99.40	99.62
	AUC	90.80	92.40	93.50	93.90	94.50	95.10	95.50	96.20	97.09
Potato	CACC	90.50	91.30	92.80	93.20	93.60	94.10	94.60	95.10	95.90
	AUC	91.30	92.20	93.40	93.90	94.40	94.90	95.30	95.70	96.04
Tomato	CACC	87.20	88.10	89.10	89.80	90.40	91.30	91.90	92.40	93.27
	AUC	90.20	90.60	91.70	92.30	92.70	93.20	93.70	94.20	95.06

Lastly, in the Tomato Leaves Dataset (TLD), the MWOADL-PLDDC technique attains increased CACC of 93.27% while the NB, RBFNN, FkNN, DT, SOM, RF, SVM, and Fuzzy_SVM models obtain decreased CACC of 87.20%, 88.10%, 89.10%, 89.80%, 90.40%, 91.30%, 91.90%, and 92.40% correspondingly. These results demonstrated the superior results of the MWOADL-PLDDC technique on the plant disease detection process.

5. Conclusion

In this written article, a novel PLD detection approach is established, named the MWOADL-PLDDC technique. The MWOADL-PLDDC technique leverages the DL model with a hyperparameter tuning strategy for PLD recognition.

It comprises three stages such as MDLDPTS feature extractor, DSAE and IWOA based classification and hyperparameter tuning. To enhance the recognition rate of the DSAE algorithm, the IWOA is enforced to alter the values of the hyperparameter of the DSAE algorithm. The simulation outcomes demonstrate the efficacy of the MWOADL-PLDDC method for precisely detecting and classifying plant ailments.

The MWOADL-PLDDC technique model exhibits high accuracy in distinguishing healthy leaves from diseased ones and accurately identifying the specific disease type. In the future, the outcome of the MWOADL-PLDDC methodology was improvised by the feature fusion and ensemble learning approaches.

References

- [1] Chitranjan Kumar, and Vipin Kumar, "Vegetable Plant Leaf Image Classification Using Machine Learning Models," *Proceedings of Third International Conference on Advances in Computer Engineering and Communication Systems*, Springer, Singapore, pp. 31-45, 2023. [[CrossRef](#)] [[Google Scholar](#)] [[Publisher Link](#)]
- [2] Deepkiran Munjal et al., "A Systematic Review on the Detection and Classification of Plant Diseases Using Machine Learning," *International Journal of Software Innovation (IJSI)*, vol. 11, no. 1, pp. 1-25, 2023. [[CrossRef](#)] [[Google Scholar](#)] [[Publisher Link](#)]
- [3] Palapati Vasavi, Arumugam Punitha, and T. Venkat Narayana Rao, "Crop Leaf Disease Detection and Classification Using Machine Learning and Deep Learning Algorithms by Visual Symptoms: A Review," *International Journal of Electrical and Computer Engineering*, vol. 12, no. 2, pp. 2079-2086, 2022. [[CrossRef](#)] [[Google Scholar](#)] [[Publisher Link](#)]
- [4] Kshyanaprava Panda Panigrahi et al., "Maize Leaf Disease Detection and Classification Using Machine Learning Algorithms," *Progress in Computing, Analytics and Networking. Advances in Intelligent Systems and Computing*, Springer, Singapore, vol. 1119, pp. 659-669, 2020. [[CrossRef](#)] [[Google Scholar](#)] [[Publisher Link](#)]
- [5] Raj Kumar et al., "A Systematic Analysis of Machine Learning and Deep Learning Based Approaches for Plant Leaf Disease Classification: A Review," *Journal of Sensors*, vol. 2023, pp. 1-13, 2023. [[CrossRef](#)] [[Google Scholar](#)] [[Publisher Link](#)]
- [6] Abu Sarwar Zamani et al., "Performance of Machine Learning and Image Processing in Plant Leaf Disease Detection," *Journal of Food Quality*, vol. 2022, pp. 1-7, 2022. [[CrossRef](#)] [[Google Scholar](#)] [[Publisher Link](#)]
- [7] Sunil S. Harakannanavar et al., "Plant Leaf Disease Detection Using Computer Vision and Machine Learning Algorithms," *Global Transitions Proceedings*, vol. 3, no. 1, pp. 305-310, 2022. [[CrossRef](#)] [[Google Scholar](#)] [[Publisher Link](#)]
- [8] Tejas Tawde et al., "Rice Plant Disease Detection and Classification Techniques: A Survey," *International Journal of Engineering Research & Technology (IJERT)*, vol. 10, no. 7, pp. 560-567, 2021. [[Google Scholar](#)] [[Publisher Link](#)]

- [9] Sandeep Kumar et al., "Leaf Disease Detection and Classification Based on Machine Learning," *2020 International Conference on Smart Technologies in Computing, Electrical and Electronics (ICSTCEE)*, Bengaluru, India, pp. 361-365, 2020. [[CrossRef](#)] [[Google Scholar](#)] [[Publisher Link](#)]
- [10] Sripada Swain, Sasmita Kumari Nayak, and Swati Sucharita Barik, "A Review on Plant Leaf Diseases Detection and Classification Based on Machine Learning Models," *Mukt Shabd Journal*, vol. 9, no. 6, pp. 5195-5205, 2020. [[Google Scholar](#)] [[Publisher Link](#)]
- [11] Seyed Mohamad Javidan et al., "Diagnosis of Grape Leaf Diseases Using Automatic K-Means Clustering and Machine Learning," *Smart Agricultural Technology*, vol. 3, pp. 1-14, 2023. [[CrossRef](#)] [[Google Scholar](#)] [[Publisher Link](#)]
- [12] M. Shantkumari, and S.V. Uma, "Grape Leaf Image Classification Based on Machine Learning Technique for Accurate Leaf Disease Detection," *Multimedia Tools and Applications*, vol. 82, no. 1, pp. 1477-1487, 2023. [[CrossRef](#)] [[Google Scholar](#)] [[Publisher Link](#)]
- [13] Eftekhar Hossain, Md. Farhad Hossain, and Mohammad Anisur Rahaman, "A Color and Texture Based Approach for the Detection and Classification of Plant Leaf Disease Using KNN Classifier," *2019 International Conference on Electrical, Computer and Communication Engineering (ECCE)*, Cox'sBazar, Bangladesh, pp. 1-6, 2019. [[CrossRef](#)] [[Google Scholar](#)] [[Publisher Link](#)]
- [14] Zhaohua Huang et al., "Grape Leaf Disease Detection and Classification Using Machine Learning," *2020 International Conferences on Internet of Things (iThings) and IEEE Green Computing and Communications (GreenCom) and IEEE Cyber, Physical and Social Computing (CPSCom) and IEEE Smart Data (SmartData) and IEEE Congress on Cybermatics (Cybermatics)*, Rhodes, Greece, pp. 870-877, 2020. [[CrossRef](#)] [[Google Scholar](#)] [[Publisher Link](#)]
- [15] Umesh Kumar Lilhore et al., "Enhanced Convolutional Neural Network Model for Cassava Leaf Disease Identification and Classification," *Mathematics*, vol. 10, no. 4, pp. 1-19, 2022. [[CrossRef](#)] [[Google Scholar](#)] [[Publisher Link](#)]
- [16] Aditi Singh, and Harjeet Kaur, "Potato Plant Leaves Disease Detection and Classification Using Machine Learning Methodologies," *IOP Conference Series: Materials Science and Engineering, 1st International Conference on Computational Research and Data Analytics (ICCRDA 2020)*, Rajpura, India, vol. 1022, pp. 2-9, 2021. [[CrossRef](#)] [[Google Scholar](#)] [[Publisher Link](#)]
- [17] Vaibhav Tiwari, Rakesh Chandra Joshi, and Malay Kishore Dutta, "Dense Convolutional Neural Networks Based Multiclass Plant Disease Detection and Classification Using Leaf Images," *Ecological Informatics*, vol. 63, 2021. [[CrossRef](#)] [[Google Scholar](#)] [[Publisher Link](#)]
- [18] S. Sai Satyanarayana Reddy et al., "Deep CNN Based Whale Optimization for Predicting the Rice Plant Disease in Real Time," *Artificial Intelligence and Data Science: First International Conference, ICAIDS 2021*, Hyderabad, India, pp. 191-202, 2022. [[CrossRef](#)] [[Google Scholar](#)] [[Publisher Link](#)]
- [19] Sundaravadivazhagan Balasubramanian et al., "An Effective Stacked Autoencoder Based Depth Separable Convolutional Neural Network Model for Face Mask Detection," *Array*, vol. 19, pp. 1-12, 2023. [[CrossRef](#)] [[Google Scholar](#)] [[Publisher Link](#)]
- [20] K. Nandhini, and G. Tamilpavai, "An Optimal Stacked ResNet-BiLSTM-Based Accurate Detection and Classification of Genetic Disorders," *Neural Processing Letters*, vol. 55, pp. 9117-9138, 2023. [[CrossRef](#)] [[Google Scholar](#)] [[Publisher Link](#)]
- [21] Yang Yu et al., "Automated Damage Diagnosis of Concrete Jack Arch Beam Using Optimized Deep Stacked Autoencoders and Multi-Sensor Fusion," *Developments in the Built Environment*, vol. 14, pp. 1-21, 2023. [[CrossRef](#)] [[Google Scholar](#)] [[Publisher Link](#)]
- [22] Tairu Oluwafemi Emmanuel, "Plant Village Dataset," *Kaggle*, 2018. [[Google Scholar](#)] [[Publisher Link](#)]